Springer

Journal of
Mechanical
Science and
Technology

Journal of Mechanical Science and Technology 22 (2008) 1008~1018

www.springerlink.com/content/1738-494x

Two-fluid Herschel-Bulkley model for blood flow in catheterized arteries

D. S. Sankar[1] and Usik Lee[2,*]

[1]*Department of Mechanical Engineering, Inha University, Incheon 402-751, Republic of Korea*
(Presently on leave from Department of Mathematics, B. S. A. Crescent Engineering College, Vandalur, Chennai-48, India)
[2]*Department of Mechanical Engineering, Inha University, 253 Yonghyun-Dong, Nam-Gu, Incheon 402-751, Republic of Korea*

(Manuscript Received February 25, 2007; Revised October 29, 2007; Accepted January 30, 2008)

Abstract

The steady flow of blood through a catheterized artery is analyzed, assuming the blood as a two-fluid model with the core region of suspension of all the erythrocytes as a Herschel-Bulkley fluid and the peripheral region of plasma as a Newtonian fluid. The expressions for velocity, flow rate, wall shear stress and frictional resistance are obtained. The variations of these flow quantities with yield stress, catheter radius ratio and peripheral layer thickness are discussed. It is observed that the velocity and flow rate decrease while the wall shear stress and resistance to flow increase when the yield stress or the catheter radius ratio increases when all the other parameters held constant. It is noticed that the velocity and flow rate increase while the wall shear stress and frictional resistance decrease with the increase of the peripheral layer thickness. The estimates of the increase in the frictional resistance are significantly much smaller for the present two-fluid model than those of the single-fluid model.

Keywords: Two-fluid model; Steady blood flow; Catheterized artery; Herschel-Bulkley fluid; Newtonian fluid

1. Introduction

With the evolution of the medical technology, catheters play a pivotal role in the modern medicine. In clinical studies, the measurement of various physiological flow quantities (such as arterial blood pressure or pressure gradient and flow velocity or flow rate) as well as the diagnosis and treatment of various arterial diseases (such as X-ray angiography, intravascular ultrasound and coronary balloon angioplasty) are done by an appropriate catheter-tool device by inserting it into an artery and positioning it in the desired part of the arterial network [1]. Catheters are even used to clear the short occlusions from the walls of the stenosed artery. The insertion of a catheter in an artery will alter the flow field, modify the pressure distribution and hence increase the flow resistance. Thus, the pressure or pressure gradient recorded by a transducer attached to the catheter will differ from that of an uncatheterized artery and it is essential to know the catheter-induced error [2]. Even, a very small angioplasty guidewire leads to a sizable increase in flow resistance. For an angioplasty guidewire, over the range of catheter radius ratio (ratio of catheter radius to coronary vessel radius) from 0.3 to 0.7 (which is currently used clinically), even for Newtonian fluid, the flow resistance increases by a large factor of 3-33 for concentric configurations [3]. For smaller infusion catheters, the flow resistance increase is less, although still appreciable. Therefore, it is meaningful to study the increase in flow resistance due to catheterization.

There have been several theoretical and experimental attempts to study the blood flow through catheterized arteries [1-8]. Back [3] and Back et al. [6] studied important hemodynamic characteristics like wall shear stress, pressure drop and frictional resistance in catheterized coronary arteries under a normal as well as a pathological situation of a stenosis present. The effect of catheterization on various flow characteristics in a curved artery was studied by

*Corresponding author. Tel.: +82 32 860 7318, Fax.: +82 32 866 1434
E-mail address: ulee@inha.ac.kr
DOI 10.1007/s12206-008-0123-4

Karahalios [9] and Jayaraman and Tiwari [10]. All of the above investigations treated blood as a Newtonian fluid.

Blood shows anomalous viscous properties. The anomalous behavior of blood is principally due to the suspension of particles in plasma. The two types of anomaly are due to 'low shear' and 'high shear' effects [11]. When blood flows through larger diameter arteries at high shear rates, it behaves like a Newtonian fluid. The apparent viscosity of blood decreases with decreasing blood vessel diameter, when measurements are made in capillaries of diameter less than $300\mu m$ [12]. This apparent dependence of viscosity on capillary radius is known as the Fahraeus-Lindqvist effect. But, when blood flows in smaller blood vessels of diameter $20\mu m - 100\mu m$, the apparent viscosity increases as the blood vessel diameter decreases and it shows a non–Newtonian character. This non–Newtonian character of blood is typical in small arteries and veins where the presence of cells induces that specific behavior.

It has been reported by Tu and Deville [13] that the assumption of Newtonian behavior of blood is acceptable for high shear rate flow, e.g., in the case of flow through large arteries. When the shear stress exceeds $100s^{-1}$, blood exhibits Newtonian behavior, and when the shear stress is less than $100s^{-1}$, blood exhibits non-Newtonian behavior [14]. It is well known that blood being suspension of cells behaves like a non-Newtonian fluid at low shear rate $(\dot{\gamma} < 10/\sec)$ and during its flow through narrow blood vessels of diameter 0.02-0.1mm [14-16]. It is true that the Casson fluid model can be used for moderate shear rates $\gamma < 10s^{-1}$ in smaller diameter tubes, whereas the Herschel–Bulkley fluid model can be used at still lower shear rate of flow in very narrow arteries where the yield stress is high [13, 17].

Dash et al. [15] analyzed the changed flow pattern in narrow artery when a catheter is inserted into it and estimated the increase in the frictional resistance in the artery due to catheterization using the Casson fluid model for both steady and pulsatile flow. Sankar and Hemalatha [18, 19] studied the steady flow of Herschel-Bulkley fluid (H-B fluid) through catheterized arteries and estimated the increase in the resistance to flow. Bugliarello and Sevilla [20] and Cokelet [21] reported that for blood flowing through narrow blood vessels, there is a peripheral layer of plasma and a core region of suspension of all the erythrocytes. Their experimentally measured velocity profiles in the tubes confirm the impossibility of representing the velocity distribution by a single-fluid model which ignores the presence of the peripheral layer which plays a crucial role in determining the flow patterns of the system. Thus, for a realistic description of blood flow, perhaps, it is more appropriate to treat the blood as a two-fluid model consisting of a core region (central layer) containing all the erythrocytes as a non-Newtonian fluid and a peripheral layer of plasma as a Newtonian fluid [22]. The analysis of two-fluid models for blood flow is better applied to small vessels such as femoral arteries, carotid, coronaries, arterioles and very small arteries of diameter 130μm-200μm where the non-Newtonian effects are expected to be significant [23]. Thus, in this paper, we have extended the single-fluid model of Sankar and Hemalatha [19] to a two-fluid model of blood.

Iida [24] reported that "The velocity profiles in the arterioles having diameter less than 0.1mm are generally explained fairly by the Casson and Herschel-Bulkley fluid models. However, the velocity profiles in the arterioles whose diameters less than 0.065mm do not conform to the Casson fluid model, but, can still be explained by the Herschel–Bulkley model". Chaturani and Ponnalagar Samy [25] and Sankar and Hemalatha [19, 26] have mentioned that for tube diameter 0.095mm, blood behaves like Herschel–Bulkley fluid rather than power law and Bingham fluids. Since the Herschel-Bulkley fluid's constitutive equation has one more parameter, namely the power law index (*n*), than the Casson fluid's constitutive equation, one can obtain more detailed information about the flow characteristics of the fluid in motion by using Herschel-Bulkley fluid rather than Casson fluid. Furthermore, the study of two-fluid models of Newtonian fluid, power law fluid and Bingham fluid can be possible by using this model as these fluid models are the particular cases of Herschel-Bulkley fluid model. Hence, it is appropriate to represent the fluid in the core region of the two-fluid model by the Herschel-Bulkley fluid model. Thus, in this paper, we study a two-fluid model for steady flow of blood through catheterized narrow arteries (of diameter 0.02mm–1mm) at low shear rates $(\dot{\gamma} < 10/\sec)$ treating the fluid in the core region as a Herschel-Bulkley fluid and the plasma in the peripheral region as a Newtonian fluid.

In this study, the effects of the catheterization, non-Newtonian nature of blood and the influence of the

peripheral layer thickness on various flow quantities are analyzed through analytical solution. The layout of the paper is as follows. The details of mathematical formulation and the method of solution are presented in sections 2 and 3, respectively. The variations of the flow quantities on yield stress, catheter radius ratio and peripheral layer thickness are discussed in section 4. The increase in the frictional resistance for different types of catheters used clinically are also estimated in section 4. The results are summarized and some clinical applications of the present study to the medical field are indicated in the concluding section 5.

2. Formulation

Consider an axially symmetric, steady, laminar and fully developed flow of blood in an artery in which a catheter is introduced coaxially, where the artery is modeled as a rigid circular tube of radius $\bar{R}$. The catheter radius is taken to be $k\bar{R}$ $(k<1)$ and the blood is modeled as a two-fluid model with the fluid in the core region of suspension of all the erythrocytes as a Herschel-Bulkley fluid (H-B fluid) and the peripheral region of plasma as a Newtonian fluid. We have used cylindrical polar coordinates $(\bar{r},\bar{\phi},\bar{z})$, where $\bar{r}$ and $\bar{z}$ denote the radial and axial coordinates and $\bar{\phi}$ is the azimuthal angle. Fig. 1 shows the flow geometry of the catheterized artery. It can be shown that the radial velocity is negligibly small in magnitude and may be neglected for the low Reynolds number flow and the pressure gradient is a function of $\bar{z}$ alone. The momentum equations in this case simplified to

$$\frac{d\bar{p}}{d\bar{z}} = -\frac{1}{\bar{r}}\frac{d}{d\bar{r}}(\bar{r}\bar{\tau}_H) \quad \text{in} \quad k\bar{R} \le \bar{r} \le \bar{R}_1 \tag{1}$$

$$\frac{d\bar{p}}{d\bar{z}} = -\frac{1}{\bar{r}}\frac{d}{d\bar{r}}(\bar{r}\bar{\tau}_N) \quad \text{in} \quad \bar{R}_1 \le \bar{r} \le \bar{R} \tag{2}$$

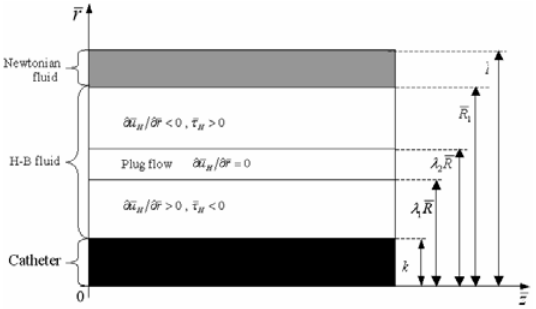

Fig. 1. Flow geometry of the catheterized artery.

where $\bar{p}$ denotes the pressure and $\bar{\tau}_H$ *and* $\bar{\tau}_N$ denote the shear stress of the Herschel-Bulkley fluid and Newtonian fluid, respectively, and $\bar{R}_1$ is the radius of the core region of the artery. The relations between the shear stress and strain rate of the fluids in motion in the core region (Herschel-Bulkley fluid) and peripheral layer (Newtonian fluid) are given by

$$\bar{\mu}_H \left|\frac{\partial \bar{u}_H}{\partial \bar{r}}\right| = \left(|\bar{\tau}_H| - \bar{\tau}_y\right)^n \text{ if } \bar{\tau}_H \ge \bar{\tau}_y \text{ and } k\bar{R} \le \bar{r} \le \lambda_1\bar{R} \text{ and } \lambda_2\bar{R} \le \bar{r} \le \bar{R}_1 \tag{3}$$

$$\frac{\partial \bar{u}_H}{\partial \bar{r}} = 0 \text{ if } \bar{\tau}_H \le \bar{\tau}_y \text{ and } \lambda_1\bar{R} \le \bar{r} \le \lambda_2\bar{R} \tag{4}$$

$$\bar{\mu}_N \left|\frac{\partial \bar{u}_N}{\partial \bar{r}}\right| = |\bar{\tau}_N| \text{ if } \bar{R}_1 \le \bar{r} \le \bar{R} \tag{5}$$

where $\bar{u}_H$, $\bar{u}_N$ are the axial component of the fluid's velocity in the core region and peripheral region; $\bar{\mu}_H$, $\bar{\mu}_N$ are the viscosities of the Herschel-Bulkley fluid and Newtonian fluid; $\bar{\tau}_y$ is the yield stress; λ_1 and λ_2 are the yield planes bounding the plug flow region. From Eq. (4), it is clear that the velocity gradient vanishes in the region where the shear stress is less than the yield stress which implies a plug flow whenever $\bar{\tau}_H \le \bar{\tau}_y$. However, the fluid behavior is indicated whenever $\bar{\tau}_H \ge \bar{\tau}_y$. The equivalent form of these relations when shear stress and strain rate have opposite signs when $|\bar{\tau}| \ge \bar{\tau}_y$ can be written as

$$\bar{\mu}_H \frac{\partial \bar{u}_H}{\partial \bar{r}} = \left(|\bar{\tau}_H| - \bar{\tau}_y\right)^n \text{ for } \frac{\partial \bar{u}_H}{\partial \bar{r}} > 0 \text{ and } \bar{\tau}_H < 0 \text{ and } k\bar{R} \le \bar{r} \le \lambda_1\bar{R} \tag{6}$$

$$\bar{\mu}_H \frac{\partial \bar{u}_H}{\partial \bar{r}} = -\left(|\bar{\tau}_H| - \bar{\tau}_y\right)^n \text{ for } \frac{\partial \bar{u}_H}{\partial \bar{r}} < 0 \text{ and } \bar{\tau}_H > 0 \text{ and } \lambda_2\bar{R} \le \bar{r} \le \bar{R}_1 \tag{7}$$

$$\bar{\mu}_N \frac{\partial \bar{u}_N}{\partial \bar{r}} = -|\bar{\tau}_N| \text{ for } \frac{\partial \bar{u}_N}{\partial \bar{r}} < 0 \text{ and } \bar{\tau}_N > 0 \text{ and } \bar{R}_1 \le \bar{r} \le \bar{R} \tag{8}$$

For $\bar{\tau}_y/|\bar{\tau}_H| \ll 1$, neglecting $\left(\bar{\tau}_y/|\bar{\tau}_H|\right)^2$ and higher powers of $\left(\bar{\tau}_y/\bar{\tau}_H\right)$, Eqs. (6) and (7) can be simplified, respectively, to

$$\bar{\mu}_H \frac{d\bar{u}_H}{d\bar{r}} = |\bar{\tau}_H|^n \left(1 - \frac{n\bar{\tau}_y}{|\bar{\tau}_H|}\right) \text{ if } \frac{d\bar{u}_H}{d\bar{r}} > 0 \text{ and } \bar{\tau}_H < 0 \text{ and } k\bar{R} \le \bar{r} \le \lambda_1\bar{R} \tag{9}$$

$$\bar{\mu}_H \frac{d\bar{u}_H}{d\bar{r}} = -|\bar{\tau}_H|^n \left(1 - \frac{n\bar{\tau}_y}{|\bar{\tau}_H|}\right) \text{ if } \frac{d\bar{u}_H}{d\bar{r}} < 0 \text{ and } \bar{\tau}_H > 0 \text{ and } \lambda_2\bar{R} \le \bar{r} \le \bar{R}_1 \tag{10}$$

Eqs. (1), (2) and (8-10) can be solved with the help of the following boundary conditions:

$$\bar{u}_H = 0 \text{ at } \bar{r} = k\bar{R} \text{ and } \bar{u}_N = 0 \text{ at } r = \bar{R} \tag{11}$$

$$\bar{u}_H = \bar{u}_N \text{ and } \bar{\tau}_H = \bar{\tau}_N \text{ at } \bar{r} = \bar{R}_1 \tag{12}$$

3. Method of solution

Let $\bar{p}_0$ be the absolute magnitude of the typical pressure gradient. Let us introduce the following non-dimensional variables:

$$\begin{aligned} &u_H = \bar{u}_H \big/ \left(\bar{p}_0 \bar{R}^2 / 2\bar{\mu}_0\right), \\ &u_N = \bar{u}_N \big/ \left(\bar{p}_0 \bar{R}^2 / 2\bar{\mu}_N\right), r = \bar{r}/\bar{R}, R_1 = \bar{R}_1/\bar{R}, \\ &z = \bar{z}/\bar{R}, \ \tau_H = \bar{\tau}_H \big/ \left(\bar{p}_0 \bar{R}/2\right), \\ &\tau_N = \bar{\tau}_N \big/ \left(\bar{p}_0 \bar{R}/2\right), \theta = \bar{\tau}_y \big/ \left(\bar{p}_0 \bar{R}/2\right) \end{aligned} \tag{13}$$

where $\bar{\mu}_0 = \bar{\mu}_H \left(2/\bar{p}_0 \bar{R}\right)^{n-1}$ is the typical viscosity coefficient having the dimension as that of the Newtonian fluid's viscosity and θ is the non-dimensional yield stress. Since, the flow is assumed as steady, the pressure gradient can be written as

$$\frac{d\bar{p}}{d\bar{z}} = -\bar{p}_0 P_S \tag{14}$$

where P_S is the non-dimensional steady state pressure gradient. Using Eqs. (13) and (14), the momentum equations (1) and (2) reduced respectively to

$$2P_S = \frac{1}{r}\frac{d}{dr}\left(r\tau_H\right) \text{ if } k \le r \le R_1 \tag{15}$$

$$2P_S = \frac{1}{r}\frac{d}{dr}\left(r\tau_N\right) \text{ if } R_1 \le r \le 1 \tag{16}$$

Similarly, using Eqs. (13) and (14), the constitutive Eqs. (9), (10), (4), and (8) are simplified, respectively, to

$$\frac{du_H}{dr} = \left|\tau_H\right|^n \left(1 - \frac{n\theta}{\left|\tau_H\right|}\right) \text{ if } \frac{du_H}{dr} > 0 \text{ and } \tau_H < 0 \text{ and } k \le r \le \lambda_1 \tag{17}$$

$$\frac{du_H}{dr} = -\left|\tau_H\right|^n \left(1 - \frac{n\theta}{\left|\tau_H\right|}\right) \text{ if } \frac{du_H}{dr} < 0 \text{ and } \tau_H > 0 \text{ and } \lambda_2 \le r \le R_1 \tag{18}$$

$$\frac{du_H}{dr} = 0 \text{ if } \tau_H \le \theta \text{ and } \lambda_1 \le r \le \lambda_2 \tag{19}$$

$$\frac{du_N}{dr} = -\left|\tau_N\right| \text{ for } \frac{\partial u_N}{\partial r} < 0 \text{ and } \tau_N > 0 \text{ and } R_1 \le r \le 1 \tag{20}$$

The boundary conditions (in the non-dimensional form) are

$$u_H = 0 \text{ at } r = k \text{ and } u_N = 0 \text{ at } r = 1 \tag{21}$$

$$u_H = u_N \text{ and } \tau_H = \tau_N \text{ at } r = R_1 \tag{22}$$

Integration of Eqs. (15) and (16) yields

$$\tau_H = P_S r + \left(C_1/r\right) \tag{23}$$

$$\tau_N = P_S r + \left(C_2/r\right) \tag{24}$$

where C_1 and C_2 are the constants of integration. From Eqs. (17-20), it is clear that the flow in $k \le r \le 1$ is a four region one, in which the core region has a flat velocity profile and hence forms the plug flow region. In this plug flow region, where the shear stress does not exceed the yield stress, the flow is not sheared in the sense that the fluid streamlines are not moving at different velocities. For mathematical representation, let this plug flow region be defined by $\lambda_1 \le r \le \lambda_2$, where $k \le \lambda_1, \lambda_2 \le 1$. Here λ_1 and λ_2 are the unknown constants to be determined. The four regions are depicted in Fig. 1. From the continuity of the shear stress along the boundary of the plug flow region, we have

$$-\tau_H\big|_{r=\lambda_1} = \theta = \tau_H\big|_{r=\lambda_2} \tag{25}$$

Using the above conditions in Eq. (23), we get

$$C_1 = -P_S \ \lambda^2 \tag{26}$$

where

$$\lambda^2 = \lambda_1 \lambda_2 \tag{27}$$

Substitution of Eq. (26) in Eq. (23) yields the shear stress for the Herschel-Bulkley fluid as

$$\tau_H = \left(P_S/r\right)\left(r^2 - \lambda^2\right) \tag{28}$$

Using Eq. (28) in Eq. (25), we can obtain

$$\lambda_2 - \lambda_1 = \left(\theta/P_S\right) = \beta \tag{29}$$

where β is the width of the plug core region. From Eqs. (22), (24) and (28), the shear stress for the Newtonian fluid can be obtained as

$$\tau_N = \left(P_S/r\right)\left(r^2 - \lambda^2\right) \tag{30}$$

The expressions for the velocity in the four regions can be obtained from Eqs. (17-22) and (28-30) and are given by

$$u_H^+(r) = P_S^n \left[\int_k^r \left(\frac{\lambda^2 - r^2}{r}\right)^n dr - n\beta \int_k^r \left(\frac{\lambda^2 - r^2}{r}\right)^{n-1} dr\right]$$

when $k \le r \le \lambda_1$ (31)

u_p = constant when $\lambda_1 \le r \le \lambda_2$ (32)

$$u_H^{++}(r) = (P_S/2)\left[1 - R_1^2 + 2\lambda^2 \log(R_1)\right] + p_S^n \left[\int_r^{R_1} \left(\frac{r^2 - \lambda^2}{r} \right)^n dr - n\beta \int_r^{R_1} \left(\frac{r^2 - \lambda^2}{r} \right)^{n-1} dr \right]$$

when $\lambda_2 \le r \le R_1$ (33)

$$u_N = (P_S/2)\left[1 - r^2 + 2\lambda^2 \log(r)\right]$$

when $R_1 \le r \le 1$ (34)

where u_p denotes the plug flow velocity, u_H^+ and u_H^{++} are the fluid's velocity in the regions $k \le r \le \lambda_1$ and $\lambda_2 \le r \le R_1$ respectively. By the continuity of the velocity distribution throughout the flow field, we have the condition

$$u_H^+(r = \lambda_1) = u_p = u_H^{++}(r = \lambda_2) \tag{35}$$

This gives

$$P_S^n \left\{ \int_k^{\lambda_1} \left(\frac{\lambda^2 - r^2}{r} \right)^n dr - \int_{\lambda_2}^{R_1} \left(\frac{r^2 - \lambda^2}{r} \right)^n dr - n\beta \left[\int_k^{\lambda_1} \left(\frac{\lambda^2 - r^2}{r} \right)^{n-1} dr - \int_{\lambda_2}^{R_1} \left(\frac{r^2 - \lambda^2}{r} \right)^{n-1} dr \right] \right\} - \frac{P_S}{2}\left[1 - R_1^2 + 2\lambda^2 \log(R_1)\right] = 0 \tag{36}$$

Using Eqs. (27) and (29) in Eq. (36), one can get

$$P_S^n \left\{ \int_k^{\lambda_1} \left(\frac{\lambda_1(\lambda_1 + \beta) - r^2}{r} \right)^n dr - \int_{\lambda_1+\beta}^{R_1} \left(\frac{r^2 - \lambda_1(\lambda_1 + \beta)}{r} \right)^n dr - n\beta \left[\int_k^{\lambda_1} \left(\frac{\lambda_1(\lambda_1 + \beta) - r^2}{r} \right)^{n-1} dr - \int_{\lambda_1+\beta}^{R_1} \left(\frac{r^2 - \lambda_1(\lambda_1 + \beta)}{r} \right)^{n-1} dr \right] \right\} - \frac{P_S}{2}\left[1 - R_1^2 + 2\lambda^2 \log(R_1)\right] = 0 \tag{37}$$

The above equation is solved numerically for λ_1 using Regula-Falsi method; the integrals are evaluated by using the Trapezoidal rule. Once λ_1 is known, λ_2 is determined using Eq. (29). The steady flow rate Q_S is given by

$$\begin{aligned} Q_S &= 8 \int_k^1 rudr \\ &= 4P_S^n \left\{ \left[-\int_k^{\lambda_1} \left(\frac{\lambda^2 - r^2}{r} \right)^n r^2 dr + \int_{\lambda_2}^{R_1} \left(\frac{r^2 - \lambda^2}{r} \right)^n r^2 dr \right] + n\beta \left[\int_k^{\lambda_1} \left(\frac{\lambda^2 - r^2}{r} \right)^{n-1} r^2 dr - \int_{\lambda_2}^{R_1} \left(\frac{r^2 - \lambda^2}{r} \right)^{n-1} r^2 dr \right] \right\} \\ &+ P_S\left[(1 - R_1^2) + 2(1 - R_1^4) - 2\lambda_2^2 (1 - R_1^2) + 4\lambda^2 (2R_1^2 - \lambda_2^2) \log(R_1) \right] \end{aligned} \tag{38}$$

The wall shear stress in the artery can be obtained from Eq. (30) and is given by

$$\tau_w = \tau_N\big|_{r=1} = P_S(1 - \lambda^2) \tag{39}$$

The frictional resistance per unit length of the artery is given by

$$\Lambda = (P_S/Q_S) \tag{40}$$

When $R_1 = 1$, the present model reduces to the single fluid model of a Herschel-Bulkley fluid, and in such a case the expressions obtained in this model for velocity, flow rate, wall shear stress and frictional resistance are in good agreement with Sankar and Hemalatha [19].

4. Results and discussions

The main objective of the present study is to analyze the effects of hydrodynamic and hemodynamic factors *in vivo* in a steady flow of blood through a catheterized artery. In particular, the effects of catheterization, non-Newtonian nature of the blood and peripheral layer thickness on the yield plane location, velocity, flow rate, wall shear stress and resistance to flow are analyzed. Since, the value of the yield stress $\bar{\tau}_y$ is 0.04 dyne/sec^2 for blood at a haematocrit of 40 [27], the non-Newtonian effects are more pronounced when the value of the yield stress increases. The range 0-0.25 is used to pronounce the effects of the non-dimensional yield stress, θ, since, this range is more suitable for all vessels through which a catheter is inserted [15, 18]. The value of the catheter radius ratio k has been taken in the range 0.1-0.6 to accommodate all the types of catheters and also to pronounce the difference in the flow quantities due

to the catheterization. It is generally observed that the typical values of the power law index n for blood flow are taken to lie between 0.9 and 1.1 and we have taken a typical values of n to be 0.95 for $n<1$ and 1.05 for $n>1$ [18]. The position of the interface between the core region and peripheral layer is denoted by R_1, and hence, the thickness of the peripheral layer is given by 1-R_1. The values of R_1 are generally taken as 0.95 and 0.985 [22, 23]. The value of the steady pressure gradient is usually taken as 1.0 [19].

4.1 Yield plane locations

The effect of finite yield stress is that the fluid exhibits solid-like behavior or plug flow in regions where the shear stress is less than the yield stress. The location of a point where the yield stress is equal to the actual shear stress is called a yield point and the locus of such points is called the yield surface or yield plane. In the case of normal tube flow, we have only one yield plane, whereas for annular flow there are two yield planes $r = \lambda_1$ and $r = \lambda_2$, and these two yield planes determine the plug flow region. From Eq. (29), it is noted that the difference $\lambda_2 - \lambda_1 = \beta$ gives the width of the plug flow region. In the case of steady flow, the yield plane locations λ_1 and λ_2 do not change during the course of motion. The variation of the yield planes λ_1 and λ_2 with yield stress θ for different values of the pressure gradient P_S with $n = R_1 = 0.95$ and $k = 0.3$ is sketched in Fig. 2. It is clear that the width β of the plug core region increases with the increasing values of the yield stress, θ. It is noticed that the width of the plug core region decreases with increase in the values of the pressure gradient for a given set of values of n, R_1 and k. It is of interest to note that the plot of the single-fluid Herschel-Bulkley model is in good agreement with Fig.3 of Sankar and Hemalatha [19]. Fig. 2 depicts the effects of the non-Newtonian nature of blood and steady pressure gradient on the yield plane location in the two-fluid model of the blood flow through a catheterized artery.

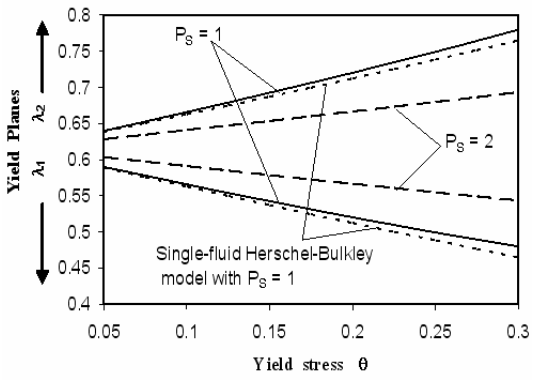

Fig. 2. Variation of yield plane with yield stress for different values of the steady pressure gradient with n = 0.95, R_1 = 0.95 and k = 0.3.

4.2 Plug flow velocity

The variation of plug flow velocity with the catheter radius ratio k for different values of the yield stress with $n = R_1 = 0.95$ and $P_S = 1$ is plotted in Fig. 3. The plug flow velocity decreases with the increase of the catheter radius ratio k. Also, the plug flow velocity decreases with the increase of the yield stress θ with the other parameters held fixed. One can note that the plug flow velocity is marginally higher for the two-fluid model than that of the single-fluid model. Fig. 3 shows the simultaneous effects of the cath-eterization and non-Newtonian nature of the blood on the plug flow velocity in the flow of a two-fluid model.

4.3 Velocity distribution

Fig. 4 depicts the velocity distribution for different values of the catheter radius ratio k and steady pressure gradient P_S with $n = R_1 = 0.95$ and $\theta = 0.1$. One can notice the plug flow around the middle of the flow region. For a given value of the steady pressure gradient and the increasing values of the catheter radius ratio k, the velocity decreases significantly, whereas the behavior is reversed (but the increase is quite high) when the pressure gradient P_S increases

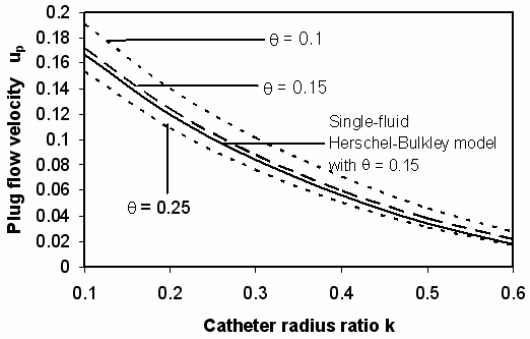

Fig. 3. Variation of plug flow velocity with catheter radius ratio for different values of yield stress with P_S = 1 and R_1 = 0.95.

while the catheter radius ratio k is kept constant. Fig. 4 depicts the effects of the catheterization and steady pressure gradient on the velocity distribution in the two-fluid model of blood flow. The velocity distribution for different values of the interface position R_1 and yield stress θ with $n = 0.95$, $P_S = 1$ and $k = 0.5$ is shown in Fig. 5. For a given value of R_1, the velocity decreases with increasing values of the yield stress θ, whereas the behavior is reversed when the thickness of the peripheral layer increases (i.e., when the value of R_1 decreases) for a fixed value of the yield stress θ. The graph of the single-fluid Herschel-Bulkley (H-B) model is in good agreement with Fig. 4 (a) of Sankar and Hemalatha [19]. Further, the velocity is considerably high near the middle of the flow for the two-fluid model than that of the single-fluid model. Fig. 5 shows the effects of peripheral layer thickness and non-Newtonian nature of blood on velocity distribution in the two-fluid model of the blood flow. Fig. 6 depicts the velocity distribution for different two-fluid models (different fluids in the core region) with $P_S = 1$, $k = 0.5$, θ = 0.1 and $R_1 = 0.95$. The velocity decreases with the increase of the power law index n when the other parameters are held constant. The two-fluid Newtonian model has the maximum velocity followed by the two-fluid power law model. One can observe the non-Newtonian effects of the blood from the flattened velocity profiles of the Herschel-Bulkley fluid.

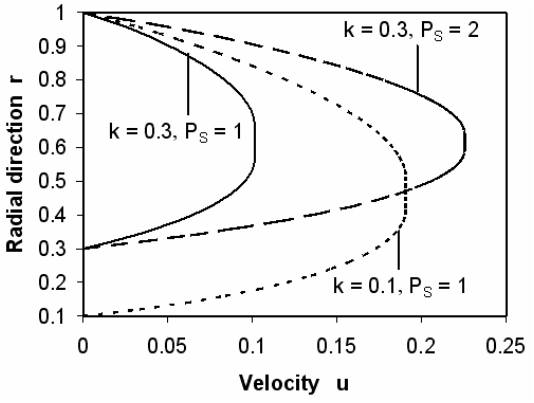

Fig. 4. Velocity distribution for different values of catheter radius ratio and steady pressure gradient with $n = R_1 = 0.95$ and θ = 0.1

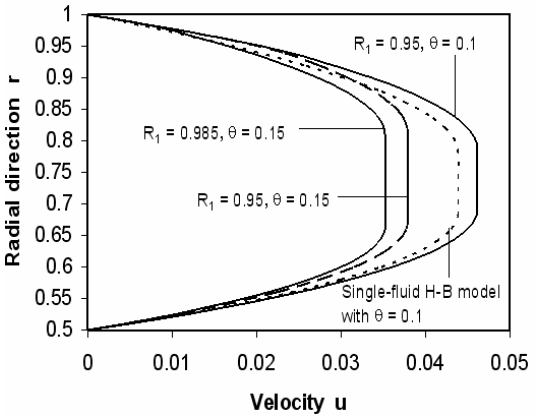

Fig. 5. Velocity distribution for different values of peripheral layer thickness and yield stress with $n = 0.95$ and $P_S = 1$

4.4 Wall shear stress

The variation of wall shear stress with the catheter radius ratio for different values of the interface position R_1 and yield stress θ with $P_S = 1$ and $n = 0.95$, is plotted in Fig. 7. The wall shear stress decreases

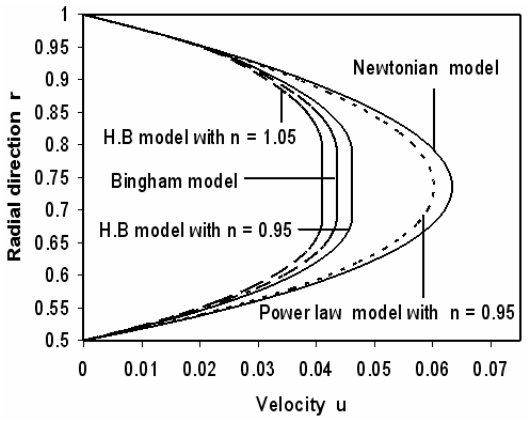

Fig. 6. Velocity distribution for different fluids in the core region with $P_S = 1$, $k = 0.5$, θ = 0.1 and $R_1 = 0.95$

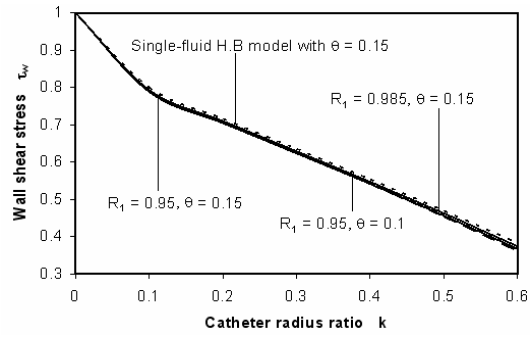

Fig. 7. Variation of wall shear stress with catheter radius ratio for different values of peripheral layer thickness and yield stress with $P_S = 1$ and $n = 0.95$.

with the increase of the catheter radius ratio k, but the decrease is steep as k increases from 0 to 0.1 and thereafter it decreases linearly. For a fixed value of R_1, the wall shear stress increases marginally with increasing values of the yield stress θ. But, the wall shear stress decreases with the increase of the peripheral layer thickness when the yield stress θ is fixed. Fig. 7 shows the simultaneous effects of the peripheral layer thickness, catheterization and non-Newtonian nature of blood on the wall shear stress of a two-fluid blood flow model.

4.5 Flow rate

Fig. 8 shows the variation of flow rate with yield stress θ for different values of the catheter radius ratio k and interface position R_1 with $n = 0.95$ and $P_S = 1$. It is clear that the flow rate decreases slowly with the increase of the yield stress θ. Furthermore, for a given value of R_1 and increasing values of the catheter radius ratio k, the flow rate decreases quite fast as k varies from 0.1 to 0.5 and decreases slowly when k increases from 0.5 to 0.7. There is a significant increase in the values of the flow rate with the increase of the peripheral layer thickness when the other parameters are kept constant. Further, it is recorded that the flow rate for the two-fluid model is quite high compared with that of the single-fluid model. Fig. 8 depicts the simultaneous effects of the catheterization and non-Newtonian nature of blood and the influence of the peripheral layer thickness on the flow rate of the two-fluid blood flow model.

4.6 Frictional resistance

The variation of the frictional resistance with the catheter radius ratio k for different values of the yield stress θ and interface position R_1 with $n = 0.95$ and $P_S = 1$ is shown in Fig. 9. The frictional resistance is seen to increase with increasing values of the catheter radius ratio k, but the increase is slow when k increases from 0.1 to 0.3 and the increase is significant when k increases from 0.3 to 0.6. It is clear that for a fixed value of R_1 and the increasing values of the yield stress θ, the resistance to flow increases marginally. It is further noted that when the peripheral layer thickness increases, the frictional resistance decreases significantly when the other parameters held constant. Interestingly, the graph of the single-fluid Herschel-Bulkley (H-B) model shows an excellent agreement with Fig. 10(a) of Sankar and Hemalatha [19]. Further, the frictional resistance is considerably lower for the two-fluid model than that of the single-fluid model. Fig. 9 shows the simultaneous effects of the catheterization and non-Newtonian nature of blood and the influence of peripheral layer thickness on the flow resistance in the two-fluid model of blood flow. Fig. 10 depicts the variation of frictional resistance with catheter radius ratio k for different two-fluid models (different fluids in the core region) with $\theta = 0.1$, $R_1 = 0.95$ and $P_S = 1$. Clearly, the fluids with the yield stress have higher resistance to flow than the fluids without the yield stress. It is noted that the resistance to flow increases with the increase in the values of the power law index n.

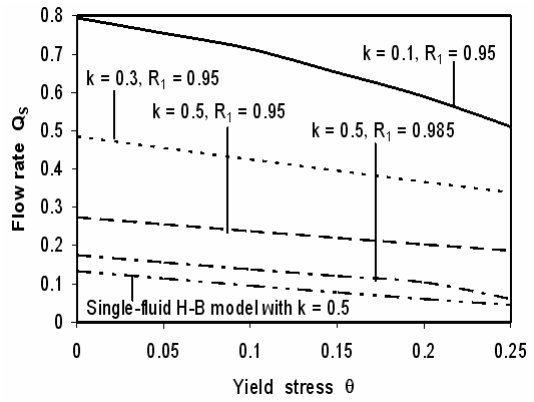

Fig. 8. Variation of flow rate with yield stress for different values of catheter radius ratio and peripheral layer thickness with $n = 0.95$ and $P_S = 1$.

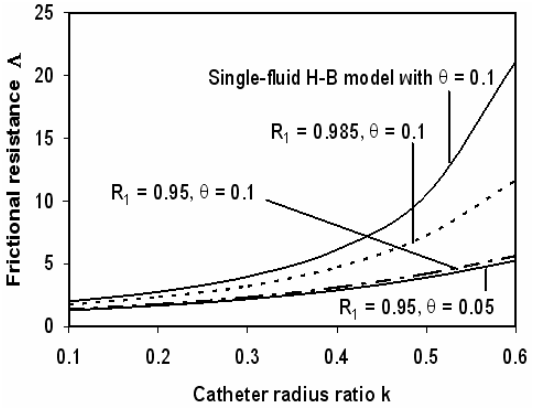

Fig. 9. Variation of frictional resistance with catheter radius ratio for different values of peripheral layer thickness and yield stress with $n = 0.95$ and $P_S = 1$.

Table 1. The estimates of the frictional resistance increase with catheter radius ratio k for different values of the yield stress θ for two-fluid and single-fluid models with effects on catheterization with $n = R_1 = 0.95$ and $P_S = 1$

K	Two-fluid model			Single-fluid model		
	θ = 0.1	θ = 0.15	θ = 0.2	θ = 0.1	θ = 0.15	θ = 0.2
0.1	1.5336	1.4330	1.4503	1.7838	1.8159	1.8523
0.2	1.9739	1.8573	1.8964	2.4513	2.5372	2.6390
0.3	2.5753	2.4386	2.5067	3.5195	3.7213	3.9718
0.4	3.4255	3.2591	3.3658	5.4274	5.9138	6.5534
0.5	4.6124	4.392	4.5342	9.2905	10.6020	12.4861
0.6	6.1550	5.8200	5.9403	18.6690	23.0930	30.5253

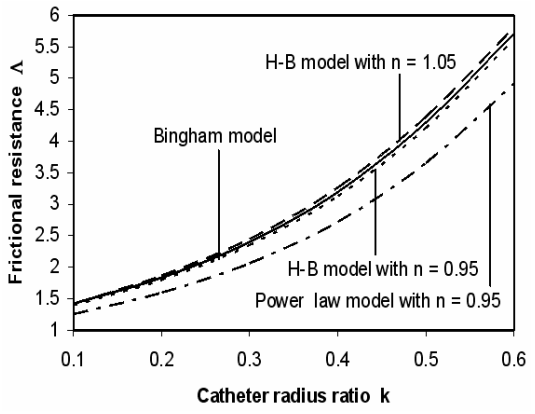

Fig. 10. Variation of frictional resistance with catheter radius ratio k for different fluids in the core region with θ = 0.1, R_1 = 0.95 and P_S = 1.

The increase in the frictional resistance due to catheterization is defined as the ratio of the frictional resistance of a fluid model in a catheterized artery for a given set of values of the parameters to the frictional resistance of the same fluid in the uncatheterized artery for the same set of values of the parameters [19]. The estimates of the increase in the frictional resistance with the catheter radius ratio k for different values of the yield stress θ for the two-fluid and single-fluid Herschel-Bulkley models with $n = R_1 = 0.95$ and $P_S = 1$ are given in Table 1. For the range 0.1-0.6 of the catheter radius ratio, the range of increase in frictional resistance for the two-fluid model are 1.53-6.16, 1.43-5.82 and 1.45-5.94 when the yield stress θ values are 0.1, 0.15 and 0.2, respectively. The corresponding increase in the frictional resistance for the single-fluid model are 1.78-18.67, 1.82-23.09 and 1.85-30.53 when the yield stress values are 0.1, 0.15 and 0.2, respectively. It is noted that the estimates of the frictional resistance for the single-fluid model show an excellent agreement with Table 6 of Sankar and Hemalatha [19]. Furthermore, the increase in the frictional resistance values is significantly much smaller for the present two-fluid model than that of the single-fluid model.

Table 2. Different types of catheters used in cardiovascular treatment, their sizes and the flow quantities measured by using them.

Type of catheter	Catheter diameter d_i (mm)	Flow quantity measured
Angioplasty catheter guidewire	0.356	Pressure drop
Coronary angioplasty catheter	1.400	Pressure distal to lesion
Guiding catheter	2.600	Pressure at coronary ostium
Doppler catheter	1.000	Velocity proximal to lesion
Coronary infusion catheter	0.660	Pressure drop across lesion

Table 3. Range of frictional resistance increase for different types of catheters for two-fluid and single-fluid models with $P_S = 1$, $R_1 = 0.95$ and θ = 0.1.

Type of catheter	Range of catheter size d_i/d_0	Two-fluid model		Single-fluid model	
		$n = 0.95$	$n = 1.05$	$n = 0.95$	$n = 1.05$
Guidewire	0.08–0.18	1.31–1.50	1.22–1.41	1.68–2.29	1.69–2.36
Infusion	0.14–0.33	1.42–1.81	1.34–1.71	2.02–3.97	2.06–4.2
Angioplasty catheter	0.3–0.6	1.74–2.56	1.65–2.46	3.52–18.67	3.7–21.33

As the possible applications of the present study, different types of catheters used in clinics, their sizes and their usage are given in Table 2 [19], where d_i is the diameter of the catheter and d_0 is the diameter of the artery. As a specific application of this study, the different types of the catheters with sizes which are generally used in the medical field, and the corresponding range of estimates of the increase in the frictional resistance for the two-fluid and single-fluid Herschel-Bulkley models with n = 0.95 and n = 1.05 are given in Table 3. It is worth noting that the range of estimates of the frictional resistance increase for the two-fluid model are very small when compared with those of the single-fluid model. Hence, it is strongly felt that the two-fluid blood flow model will have more applicability than the single-fluid blood

flow model in clinical use.

5. Conclusions

This study brings out many interesting fluid mechanical phenomena due to the catheterization and presence of the peripheral layer. Blood has been modeled as a two-fluid model with the core region of suspension of all the erythrocytes as a Herschel-Bulkley fluid and the plasma in the peripheral region as a Newtonian fluid. The artery is assumed as a rigid wall in which the catheter is inserted coaxially. It is noted that the velocity and flow rate decrease, while the wall shear stress and resistance to flow increase when the yield stress or the catheter radius ratio increases with all the other parameters held constant. Furthermore, the velocity and flow rate increase and the wall shear stress and frictional resistance decrease with the increase of the peripheral layer thickness. The width of the plug flow region increases with the increase of the yield stress, and the reverse behavior is noticed when the steady state pressure gradient increases when all the other parameters are kept fixed.

Since the difference between the estimates of the two-fluid model and single-fluid model is substantial, one can expect a marked increase in the flow of the two-fluid model. Hence, the modeling of the blood flow through catheterizes narrow arteries by a single-fluid model could not be appropriate. The increase in the resistance to flow is an important factor in the studies of blood rheology and is considerably very low for the present model; therefore, it is believed that the use of the present model for analyzing the blood flow may give more reliable data. By using the present model, physicians can be more accurate in predicting the post catheterization flow quantities. In view of the above discussions, it is concluded that the present study could be very useful for analyzing the blood flow through catheterized arteries.

References

[1] G. Jayaraman and R. K. Dash, Numerical study of flow in a constricted curved annulus: an application to flow in a catheterized artery, *Journal of Engineering Mathematics,* 40 (2001) 355-376.

[2] P. Daripa and R. K. Dash, A numerical study of pulsatile blood flow in an eccentric catheterized artery using a fast algorithm, *Journal of Engineering Mathematics,* 42 (2002) 1-22.

[3] L. H. Back, Estimated mean flow resistance increase during coronary artery catheterization, *Journal of Biomechanics,* 27 (1994) 169-175.

[4] D. A. MacDonald, Pulsatile flow in a catheterized artery, *Journal of Biomechanics,* 19 (1986) 239-249.

[5] L. H. Back and T. A. Denton, Some arterial wall shear stress estimates in coronary angioplasty, *Advances in Bioengineering,* 22 (1992) 337-340.

[6] L. H. Back, E. Y. Kwack and M. R. Back, Flow rate-pressure drop relation in coronary angioplasty: catheter obstruction effect, *ASME Journal of Biomechanical Engineering,* 118 (1996) 83-89.

[7] R. K. Dash, G. Jayaraman and K. N. Metha, Flow in a catheterized curved artery with stenosis, *Journal of Biomechanics,* 32 (1999) 49-61.

[8] A. Sarkar and G. Jayaraman, Correction to flow rate-pressure drop relation in coronary angioplasty: steady streaming effect, *Journal of Biomechanics,* 31 (1998) 781- 791.

[9] G. T. Karahalios, Some possible effects of a catheter on the arterial wall, *Medical Physics,* 17 (1990) 922-925.

[10] G. Jayaraman and K. Tiwari, Flow in a catheterized curved artery, *Medical and Biological Engineering and Computing,* 33 (1995) 1-6.

[11] S. Chien, S. Usami and R. Skalak, 1984, Blood flow in small tubes, In Renkins E. M., Michel C. C. (Eds), *American Physiological Society Handbook of Physiology*, Section 2, *The Cardiovascular system*, Vol. 4, Bethesda MD: American Physiological Society (1984) 217-249.

[12] R. Fahraeus and R. Lindqvist, Viscosity of Blood in Narrow Capillary Tubes, *American Jour-nal Physiology,* 96 (1931) 562-568.

[13] C. Tu and M. Deville, Pulsatile flow of non-Newtonian fluids through arterial stenosis, *Journal of Biomechanics,* 29 (1996) 899-908.

[14] D. Liepsch, T. Kamada and A. Pall, Two phase flow measurements in glass tube models with a laser-doppler–anemometer, In S. Hosoda, T. Yaginuma, M. Sugawara et al (eds), *Recent Progress in Cardiovascular Mechanics,* Chur, Switzerland: Hanwood Academic Publishers (1994) 21-48.

[15] R. K. Dash, G. Jayaraman and K. N. Metha, Estimation of increased flow resistance in a narrow catheterized artery–a theoretical model, *Journal of Biomechanics,* 29 (1996) 917-930.

[16] D. S. Sankar and K. Hemalatha, Pulsatile flow of Herschel-Bulkley fluid through stenosed arteries-a mathematical model, *International Journal of Non-*

Linear Mechanics, 41 (2006) 979-990.

[17] G. W. Scott Blair and D. C. Spanner, An Introduction to Biorheology, Elsevier Scientific Publication Co., Amsterdam, Oxford and New York (1974).

[18] D. S. Sankar and K. Hemalatha, Pulsatile flow of Herschel-Bulkley fluid through catheterized arteries-a mathematical model, *Applied Mathematical Modeling,* 31 (2007a) 1497-1517.

[19] D. S. Sankar and K. Hemalatha, A non-Newtonian fluid flow model for blood flow through a catheterized artery-steady flow, *Applied Matheatical Modeling,* 31 (2007b) 1847-1864.

[20] G. Bugliarello and J. Sevilla, Velocity distribution and other characteristics of steady and pulsatile blood flow in fine glass tubes, *Biorheology,* 7 (1970) 85-107.

[21] G. R. Cokelet, The rheology of human blood, In Fung, Y. C. (Eds), *Biomechanics,* Prentice-Hall, Englewood Cliffs, N.J. (1972).

[22] D. S. Sankar and U. Lee, Two-phase non-linear model for the flow through stenosed blood vessels, *Journal of Mechanical Science and Technology* 21 (2007) 678-689.

[23] V. P. Srivastava and M. Saxena, Two-layered model of Casson fluid flow through stenotic blood vessels: applications to the cardiovascular system, *Journal of Biomechanics,* 27 (1994) 921-928.

[24] N. Iida, Influence of plasma layer on steady blood flow in micro vessels, *Japanese Journal of Applied Physics,* 17 (1978) 203-214.

[25] P. Chaturani and R. Ponnalagar Samy, Pulsatile flow of a Casson fluid through stenosed arteries with application to blood flow, *Biorheology,* 23 (1986) 499-511.

[26] D. S. Sankar and K. Hemalatha, Non-Linear mathematical models for blood flow through tapered tubes, *Applied Mathematics and Computation,* 188 (1) (2007c) 567-582.

[27] E. W. Merrill, Rheology of human blood and some speculations on its role in vascular homeostasis, In: *Biomechanical Mechanisms in Vascular Homeostasis and Intravascular Thrombus,* P. N. Sawyer, eds., Appleton Century Crafts, New York (1965).